DOKUZ EYLÜL UNIVERSITY

GRADUATE SCHOOL OF NATURAL AND APPLIED SCIENCES

COHERENT NEUTRINO NUCLEUS SCATTERING

by

Mahfuz KAYA

October, 2019

İZMİR

COHERENT NEUTRINO NUCLEUS SCATTERING

A Thesis Submitted to the
Graduate School of Natural and Applied Sciences of Dokuz Eylül University
In Partial Fulfillment of the Requirements for the Degree of
Master of Science in Physics

by
Mahfuz KAYA

October, 2019
İZMİR

M.Sc THESIS EXAMINATION RESULT FORM

We have read the thesis entitled **" COHERENT NEUTRINO NUCLEUS SCATTERING"** completed by **MAHFUZ KAYA** under supervision of **PROF. DR. MUHAMMED DENİZ** and we certify that in our opinion it is fully adequate, in scope and in quality, as a thesis for the degree of Master of Science.

Prof. Dr. Muhammed DENİZ

Supervisor

Prof. Dr. Saime Kerman

(Jury Member)

Doç. Dr. Ayşe KÜÇÜKARSLAN

(Jury Member)

Prof. Dr. Kadriye ERTEKİN

Director

Graduate School of Natural and Applied Sciences

ACKNOWLEDGMENTS

This thesis is finished with help and inspiration of many people. Firstly, I would like to thank to my supervisor, Prof. Dr. Muhammed DENİZ for leading during my research. He illuminates my way and this thesis comes to life.

I would like to express my sincere gratitude to Prof. Dr. Saime KERMAN for contributing my research with her precious help. Her vision and guidance lead me to finish this work.

I want to express my deep gratefulness to my family for their sacrifices and financial help for me .

Also I want to send very warm thanks to my friends Koray DEMİR, Umut YILMAZ and Serdal ACAR for their constant encouragement and financial support during this research.

My final thanks go for all people who support me in this research.

Mahfuz KAYA

COHERENT NEUTRINO NUCLEUS SCATTERING

ABSTRACT

Coherent neutrino nucleus scattering is one of the fundamental process in the Standard Model. In this process neutrinos scatter off nucleus as a whole and nucleus stays in its ground state. During the process, the kinetic energy of neutrino decreases. In this process no new particles are created. This process can be probed with measuring nuclear recoil energy. This reaction has never been observed at low energy regions yet. Cross section for this process is larger than the other neutrino interactions.

Keywords: Standard model, beyond the standard model, neutrino, nucleus, neutrino-nucleus coherent scattering, TEXONO

KOHERENT NÖTRİNO NÜKLEUS SAÇILIMI

ÖZ

Koherent elastik nötrino nükleus saçılımı Standart Modelin temel proseslerinden birisidir. Bu proseste nötrinolar çekirdekten bir bütün olarak saçılırlar ve çekirdek temel durumunda kalır. Bu işlem sırasında nötrino kinetik enerjisini kaybeder. Bu reaksiyon düşük enerjilerde henüz gözlenmedi. Bu işlem sırasında yeni parçacıklar oluşmaz. Bu prosesi nükler geri tepme enerjini ölçerek saptayabiliriz. Bu işlem için tesir kesiti diğer nötrino reaksiyonlarının tesir kesitlerinden daha büyüktür.

Anahtar Kelimeler: Standart model, standart model ötesi, nötrino, nükleus, koherent nötrino-nükleus saçılması, TEXONO

CONTENTS

Page

LIST OF FIGURES

Page

LIST OF TABLES

Page

CHAPTER ONE
INTRODUCTION AND MOTIVATION

Neutrino interactions are fundamental processes in the Standard Model. Coherent neutrino nucleus scattering has not been observed at low energy ranges yet. In this thesis some prospects will be shown for that process. The study will focus on degree of coherency and how it changes with the interaction energy. Energy range for incoming neutrino is up to 50 MeV. After that scale neutrino interacts with nucleons, so process becomes neutrino nucleon scattering. For investigation three samples (Ar, Ge, and Xe) are chosen. All these there elements can be used in an experiment as a target nuclei.

A parameter will be defined which determines degree of coherency in neutrino nucleus scattering. The same parameter will be used to investigate which flux is suitable for experiments to detect the process.

Detection of coherent neutrino nucleus scattering may open the doors for dark matter research and help to understand supernova collapse mechanism. It is also good probe to understand nuclear form factors and to study neutron distribution in a nuclei.

1.1 History of Neutrino

Pauli's letter (Ramond, 2019),

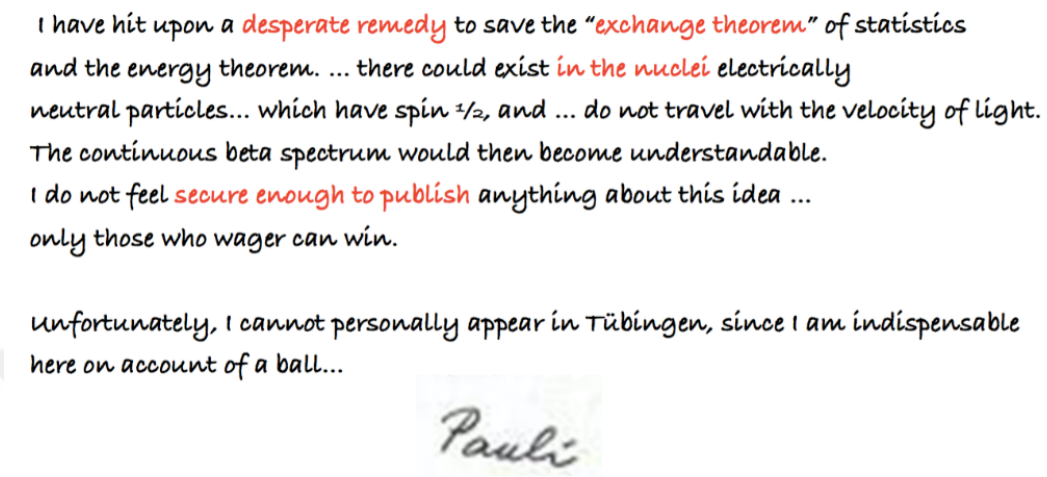
I have hit upon a desperate remedy to save the "exchange theorem" of statistics
and the energy theorem. ... there could exist in the nuclei electrically
neutral particles... which have spin ½, and ... do not travel with the velocity of light.
The continuous beta spectrum would then become understandable.
I do not feel secure enough to publish anything about this idea ...
only those who wager can win.

Unfortunately, I cannot personally appear in Tübingen, since I am indispensable
here on account of a ball...

Pauli

Figure 1.1 Pauli's letter

Neutrino's prediction started with beta decay problem.

$$A(Z,N) \rightarrow A(Z+1,N-1) + e^{-} \tag{1.1}$$

In this process daughter nucleus has less mass than the parent. It was expected that mass difference taken by electron as kinetic energy. But, electron always carried off less energy than expected. Instead of all electrons having the same energy, there was a continuous distribution. In December 1930 a letter was written by Wolfgang Pauli to a conference in Tübingen. He proposed the existence of a neutral particle of spin 1/2 emitted alongside the electron in beta decay. Pauli named that particle neutron at first. After neutron discovery by Chadwick in 1932, Fermi named Pauli's particle as neutrino. After neutrinos discovery, beta decay take the fallowing form :

$$A(Z,N) \rightarrow A(Z+1,N-1) + e^{-} + \bar{\nu}_e \tag{1.2}$$

1.2 Neutrino Sources

1.2.1 Rector Neutrinos

Reactors produce neutrinos due to the decay of the fission products. Reactor neutrinos have high flux and low energy (up to 8 MeV). The reactor neutrinos flux consist of electron anti-neutrinos. Due to low energy of reactor neutrinos recoil of a nucleus expected to be in keV region.

1.2.2 Solar Neutrinos

Nuclear fusion in the sun produces neutrinos. All of the neutrinos produced in the sun are electron neutrinos. The highest energy (up to 16 MeV) solar neutrinos produced from the β decay of boron-8 as fallows (Thomson, 2013):

$$ {}^{4}_{2}He + {}^{3}_{2}He \rightarrow {}^{7}_{4}Be + \gamma \tag{1.3} $$

$$ {}^{7}_{4}Be + p \rightarrow {}^{8}_{5}B + \gamma \tag{1.4} $$

with the β decay,

$$ {}^{8}_{5}B \rightarrow {}^{8}_{4}B^{*} + e^{+} + \nu_{e} \tag{1.5} $$

Solar neutrinos are suitable for coherent neutrino nucleus scattering detection with their energy range.

1.2.3 Stopped Pion Neutrinos

Stopped pion neutrinos produced by bombarding protons on a heavy nuclei. In that process π^{+} and π^{-} are created. π^{-} get captured by positively charged medium. π^{+}

decays at rest.

$$\pi^+ \rightarrow \mu^+ + \nu_\mu \tag{1.6}$$

$$\mu^+ \rightarrow e^+ + \bar{\nu_\mu} + \nu_e \tag{1.7}$$

Equation (1.6) is a two body decay and produce monochromatic ν_μ's at 29.9 MeV. Equation (1.7) is a three body decay and enrgy range is between 0 and $m_\mu/2$ (up to 52.8 MeV). For lepton masses see Table A.3.

1.2.4 Neutrino Fluxes

Neutrino fluxes refs.(AvignoneIII & Efremenko, 2003), (Scholberg, 2006)

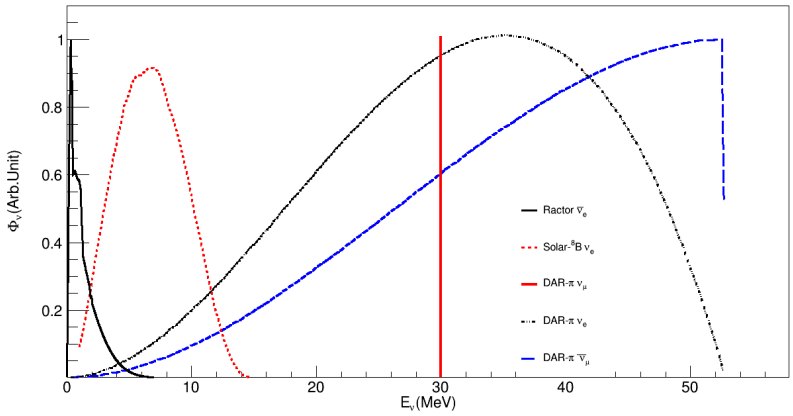

Figure 1.2 Neutrino fluxes

Neutrino spectra normalized by their maxima. Sources are reactor $\bar{\nu_e}$ from TEXONO, solar boron-8 (^8B), and $DAR-\pi$ ($\nu_\mu, \nu_e, \bar{\nu_\mu}$) from SNS.

1.3 Detection of CEvENS at SNS

In 2017 COHERENT collaboration reported observation of coherent neutrino-nucleus scattering. Collaboration has used mid-range energy neutrino fluxes from decay at rest pions (Akimov et al., 2017).

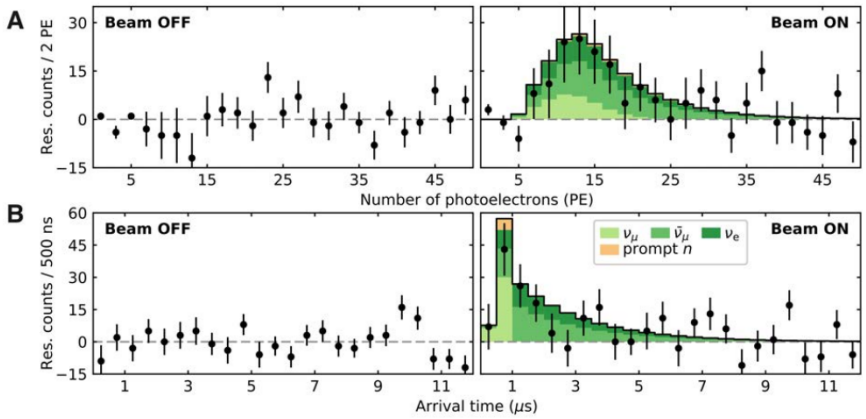

Figure 1.3 Observation of coherent elastic neutrino-nucleus scattering.

CHAPTER TWO
THEORY OF NEUTRINO NUCLEUS SCATTERING

2.1 Neutrino Interactions

2.1.1 Electro-weak Lagrangian

Electroweak lagrangian (Beringer et al., 2012) :

$$\begin{aligned}\mathscr{L}_{EW} = & - e\sum_i Q_i \bar{\psi}_i \gamma^\mu \psi_i A_\mu \\ & - \frac{g}{2}\sqrt{2}\sum_i \overline{\Psi_i}\gamma^\mu(1-\gamma^5)(T^+W_\mu^+ + T^-W_\mu^-)\Psi_i \\ & - \frac{g}{2\cos\theta_W}\sum_i \bar{\psi}_i\gamma^\mu(g_V^i - g_A^i)\psi_i Z_\mu \end{aligned} \tag{2.1}$$

The ψ_i are fermion fields, and Ψ_i are fermion doublets $\begin{pmatrix} \nu_{l_i} \\ l_i \end{pmatrix}$ and $\begin{pmatrix} u_i \\ d_i' \end{pmatrix}$

where $d' = \sum_i V_{ij} d_j$ with V the Cabibbo-Kobayashi-Maskava (CKM) matrix.

In (2.1), electro-magnetic interactions are represented in the first term with photon field A_μ. Photon field has no mass. Charge of fermions denoted with Q_i. The second line shows weak interactions. Weak boson fields (charged) denoted with W_μ^+ and W_μ^- with mass M_W. The rising and lowering operators of weak iso-spin denoted with $T^\pm$. The third line shows natural part of weak interactions with field boson Z_μ and have mass $M_Z = \frac{M_W}{\cos\theta_w}$.

2.1.2 Currents From Electro-weak Lagrangian

$$J^{\mu}_{EM} = \sum_i Q_i \bar{\psi}_i \gamma^{\mu} \psi_i \tag{2.2}$$

$$J^{\mu}_{CC} = \sum_i \overline{\Psi}_i \gamma^{\mu} (1-\gamma^5)(T^+ + T^-)\Psi_i \tag{2.3}$$

$$J^{\mu}_{NC} = \sum_i \bar{\psi}_i \gamma^{\mu} (g^i_V - g^i_A)\psi_i \tag{2.4}$$

The chiral form of neutral current is (Lindner et al., 2017) :

$$J^{\mu}_{NC} = \sum_i 2\left(g^i_L \bar{\psi^L_i} \gamma^{\mu} \psi^L_i\right) + \sum_i 2\left(g^i_R \bar{\psi^R_i} \gamma^{\mu} \psi^R_i\right) \tag{2.5}$$

The chiral projections are:

$$\psi^L_i = P_L \psi_i = \frac{1-\gamma^5}{2}\psi_i \tag{2.6}$$

$$\psi^R_i = P_R \psi_i = \frac{1+\gamma^5}{2}\psi_i \tag{2.7}$$

and

$$g^i_V = g^i_L + g^i_R \tag{2.8}$$

$$g^i_A = g^i_L - g^i_R \tag{2.9}$$

At the low energy limit:

$$\frac{g_{\mu\nu} - \dfrac{p_\mu p_\nu}{M^2_Z}}{q^2 - M^2_Z} = -\frac{g_{\mu\nu}}{M^2_Z} \tag{2.10}$$

With that, natural current with G_F as Fermi constant can be written as fallows (Lindner et al., 2017):

$$\mathscr{L}_{NC} = \frac{G_F}{\sqrt{2}} J^{\mu}_{NC} J_{NC\mu} \tag{2.11}$$

2.2 Evaluating the Amplitude Square ($|M|^2$)

2.2.1 The Amplitude $\mathscr{M}$

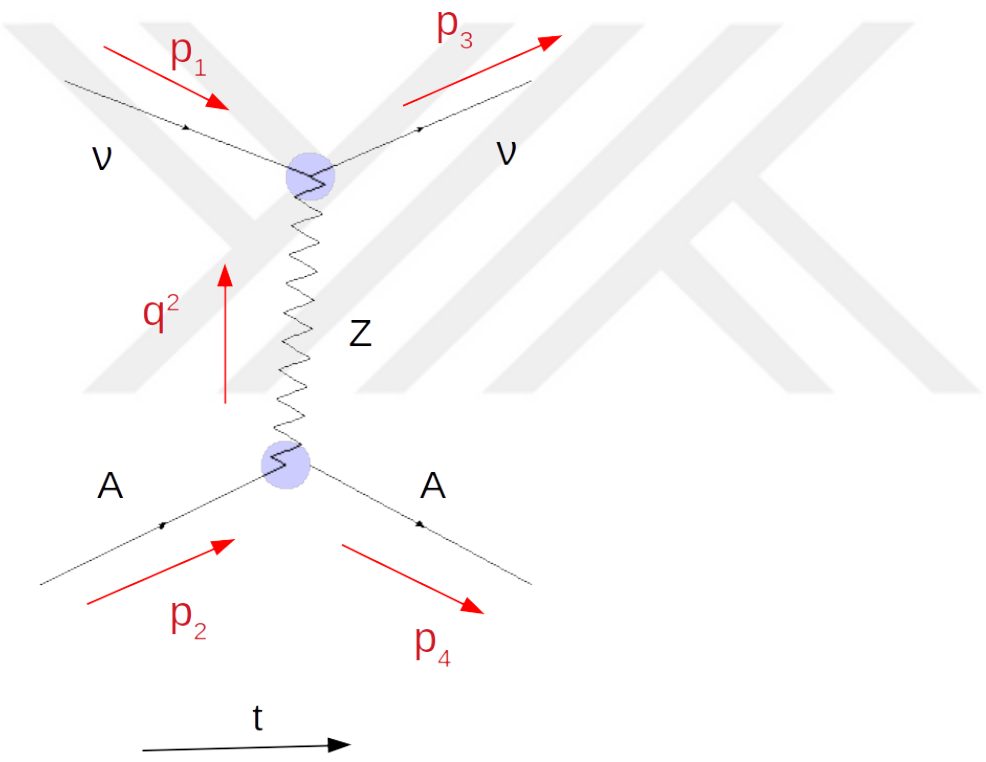

Figure 2.1 Feynman diagram for νA process

Assumptions for nucleus:

- Nucleus must be even-even number for to be in graund state.
- Nucleus must be spherical symmetric then interaction does not violate parity.

After applying Feynman rules the amplitude becomes as:

$$i\mathscr{M}_{ss'} = -i\frac{g}{2\cos\theta_W} g_L^{\nu} \bar{u}_{s'}(p_3)\gamma^{\mu}(1-\gamma^5)u_s(p_1) \left[-i\frac{g_{\mu\nu} - \dfrac{p_\mu p_\nu}{M_Z^2}}{q^2 - M_Z^2} \right] J_{nuc}^{\nu} \tag{2.12}$$

The initial and final states of particles are represented by $u_s(p_1)$ and $\bar{u}_{s'}(p_3)$. J_{nuc}^{ν} is nuclear current.

J_{nuc}^{ν} can be written as:

$$J_{nuc}^{\nu} = \lambda \left(p_2 + p_4\right)^{\nu} \tag{2.13}$$

Here λ is weak coupling strength. To find value of λ, the neutral current part of $\mathscr{L}_{EW}$ will be considered.

Since nucleus include only quarks, J_{NC}^{μ} will contribute to J_{nuc}^{ν} with quark part. Assumptions for parity conservation:

$$\bar{u}^L \gamma^{\mu} u^L = \bar{u}^R \gamma^{\mu} u^R \tag{2.14}$$

$$\bar{d}^L \gamma^{\mu} d^L = \bar{d}^R \gamma^{\mu} d^R \tag{2.15}$$

For the d (down quark) and u (up quark) part of J_{NC}^{μ}:

$$J_{NC}^{\mu} = g_V^U \bar{u}\gamma^{\mu} u + g_V^D \bar{d}\gamma^{\mu} d \tag{2.16}$$

Contributions to weak couplings are $\frac{g}{2C_W} g_V^U$ from up quark and $\frac{g}{2C_W} g_V^D$ from down quark.

Here $C_W = \cos\theta_W$ and $S_W^2 = \sin^2\theta_W$.

A nucleus $A(Z,N)$ has $n^D = 2N+Z$ d quarks and $n^U = 2Z+N$ u quarks. The weak coupling constant λ becomes:

$$\begin{aligned}
\lambda &= n^U \frac{g}{2C_W} g_V^U + n^D \frac{g}{2C_W} g_V^D \\
&= \frac{g}{2C_W}\left[n^U\left(\frac{1}{2}-\frac{4}{3}S_W^2\right)+n^D\left(\frac{1}{2}+\frac{2}{3}S_W^2\right)\right] \\
&= \frac{g}{2C_W}\frac{1}{2}\underbrace{\left[\left(1-4S_W^2\right)Z-N\right]}_{Q_W} \\
&= \frac{g}{2C_W}\frac{1}{2}Q_W
\end{aligned} \tag{2.17}$$

Here Q_W is weak charge for nucleus. In this current nucleus considered as a point-like particle. For counting inner structure of nucleus, the current will be multiplied with a form factor $F(q^2)$:

$$J_{nuc}^{\nu} = \lambda\,(p_2+p_4)^{\nu}\,F(q^2) \tag{2.18}$$

$$\tag{2.19}$$

Inserting this result in (2.12) :

$$i\mathscr{M}_{ss'} = -\frac{g^2}{8\cos^2\theta_W} Q_W g_L^{\nu} \bar{u}_{s'}(p_3)\gamma^{\mu}(1-\gamma^5)u_s(p_1)\left[\frac{g_{\mu\nu}-\dfrac{p_\mu p_\nu}{M_Z^2}}{q^2-M_Z^2}\right](p_2+p_4)_{\mu}\,F(q^2) \tag{2.20}$$

At the low energies, when $q^2 \ll M_Z^2$, the Z boson propagator becomes:

$$\frac{g_{\mu\nu}-\dfrac{p_\mu p_\nu}{M_Z^2}}{q^2-M_Z^2} = -\frac{g_{\mu\nu}}{M_Z^2} \tag{2.21}$$

With that approximation the interaction can be written in the form of eqn (2.11)

$$i\mathscr{M}_{ss'} = -\frac{g^2}{8\cos^2\theta_W M_Z^2} Q_W g_L^{\nu} \bar{u}_{s'}(p_3)\gamma^{\mu}(1-\gamma^5)u_s(p_1)\,(p_2+p_4)_{\mu}\,F(q^2) \tag{2.22}$$

Since $M_W = M_Z\cos\theta_W$ and $G_F/\sqrt{2} = g^2/8M_W^2$:

$$i\mathscr{M}_{ss'} = -\frac{G_F}{\sqrt{2}} Q_W g_L^{\nu} \bar{u}_{s'}(p_3)\gamma^{\mu}(1-\gamma^5)u_s(p_1)\,(p_2+p_4)_{\mu}\,F(q^2) \tag{2.23}$$

2.2.2 The Amplitude Square $|\mathscr{M}|^2$

To get $|\mathscr{M}|^2$, $\mathscr{M}$ with $\mathscr{M}^{\dagger}$ will be multipied and summed over final states.

$$\begin{aligned}\sum_{ss'}(\mathscr{M}\mathscr{M}^{\dagger}) = \frac{G_F^2}{2} Q_W^2 F^2 (g_L^{\nu})^2 (p_2+p_4)_{\mu}(p_2+p_4)_{\nu} \\ \times \bar{u}^{s'}(p_1)\gamma^{\mu}(1-\gamma^5)u^{s}(p_3)\bar{u}^{s}(p_3)\gamma^{\nu}(1-\gamma^5)u^{s'}(p_1)\end{aligned} \tag{2.24}$$

Now Casimir's trick and completeness relation will be used.

$$\begin{aligned}&\sum[\bar{u}_1\gamma^{\mu}v_2][\bar{v}_2\gamma^{\nu}u_1] \\ &= \sum_{\sigma_1\sigma_2} \bar{u}_{1\alpha}\gamma^{\mu}_{\alpha\beta} v_{2\beta}\bar{v}_{2\gamma}\gamma^{\nu}_{\gamma\delta}\underbrace{u_{1\delta}}_{\longleftarrow}\end{aligned} \tag{2.25}$$

Now $u_{1\delta}$ can be moved to the front. It is just a number so it commutes with everything.

$$\sum_{\sigma_1\sigma_2} u_{1\delta}\bar{u}_{1\alpha}\gamma^{\mu}_{\alpha\beta} v_{2\beta}\bar{v}_{2\gamma}\gamma^{\nu}_{\gamma\delta} \tag{2.26}$$

Using completeness relation:

$$\sum_{\sigma_1} u_{1\delta}\bar{u}_{1\alpha} = (\not{p}_3 + m_1)_{\delta\alpha} \tag{2.27}$$

$$\sum_{\sigma_1} v_{2\beta}\bar{v}_{2\gamma} = (\not{p}_4 - m_2)_{\beta\gamma} \tag{2.28}$$

Which turns the sum into:

$$\begin{aligned}&(\not{p}_3 + m_1)_{\delta\alpha}\gamma^{\mu}_{\alpha\beta}(\not{p}_4 - m_2)_{\beta\gamma}\gamma^{\nu}_{\gamma\delta}\\ &= Tr[(\not{p}_3 + m_1)\gamma^{\mu}(\not{p}_4 - m_2)\gamma^{\nu}]\end{aligned} \tag{2.29}$$

2.2.3 Trace Calculation of Neutrino Part

$$\sum_{ss'} = \bar{u}^{s'}_{\alpha}(p_1)\gamma^{\mu}_{\alpha\beta}(1-\gamma^5)_{\beta\gamma}u^{s}_{\gamma}(p_3)\bar{u}^{s}_{\delta}(p_3)\gamma^{\nu}_{\delta\sigma}(1-\gamma^5)_{\sigma\rho}u^{s'}_{\rho}(p_1) \tag{2.30}$$

Taking $u^{s'}_{\rho}(p_1)$ to the front and using completeness relation: u^{s} and $u^{s'}$ are particles,

$$\sum_{s'} u^{s'}_{\rho}(p_1)\bar{u}^{s\prime}_{\alpha}(p_1) = (\not{p}_1 + m)_{\rho\alpha} \tag{2.31}$$

$$\sum_{s} u^{s}_{\gamma}(p_3)\bar{u}^{s}_{\delta}(p_3) = (\not{p}_3 + m)_{\gamma\delta} \tag{2.32}$$

Sum turns into:

$$\begin{aligned}&(\not{p}_1 + m)_{\rho\alpha}\gamma^{\mu}_{\alpha\beta}(1-\gamma^5)_{\beta\gamma}(\not{p}_3 + m)_{\gamma\delta}\gamma^{\nu}_{\delta\sigma}(1-\gamma^5)_{\sigma\rho}\\ &= Tr[\not{p}_1\gamma^{\mu}(1-\gamma^5)\not{p}_3\gamma^{\nu}(1-\gamma^5)] + Tr[m^2\gamma^{\mu}(1-\gamma^5)\gamma^{\nu}(1-\gamma^5)]\end{aligned} \tag{2.33}$$

Getting result from FeynCalc:

$$Tr = 8(p_1^{\mu}p_3^{\nu} + p_1^{\nu}p_3^{\mu} - g^{\mu\nu}p_1 \bullet p_3 - i\varepsilon^{\rho\mu\sigma\nu}p_{1\rho}P_{3\sigma}) \tag{2.34}$$

Multiplying this result by $(p_2+p_4)_\mu((p_2+p_4)_\nu$:

$$|\mathscr{M}|^2 = 4G_F^2 Q_W^2 F^2(q^2)(g_L^\nu)^2[2p_1 \bullet (p_2+p_4)p_3 \bullet (p_2+p_4) \\ -(p_2+p_4)^2 p_1 \bullet p_3 - \underbrace{i\varepsilon^{\rho\mu\sigma\nu} p_{1\mu}(p_1+p_2)_\nu P_{3\rho}(p_2+p_4)_\sigma}_{=0}] \tag{2.35}$$

$|\mathscr{M}|^2$ become:

$$|\mathscr{M}|^2 = 8G_F^2 Q_W^2 F^2(q^2)(g_L^\nu)^2[(p_1 \bullet p_2)(p_3 \bullet p_2) + (p_1 \bullet p_2)(p_3 \bullet p_4) \\ +(p_1 \bullet p_4)(p_3 \bullet p_2) + (p_1 \bullet p_4)(p_3 \bullet p_4) - (M^2 + p_2 \bullet p_4)(p_1 \bullet p_3)] \tag{2.36}$$

2.2.4 Calculation of Kinematics

In the lab frame:

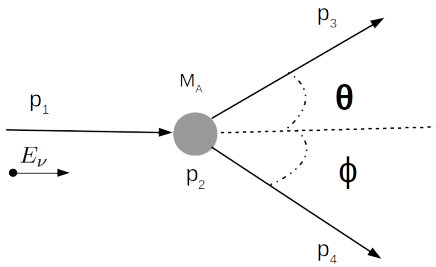

Figure 2.2 Two body scattering in lab frame

$$p_1 = (E_\nu, \vec{p}_1) \tag{2.37}$$

$$p_2 = (M_A, 0) \tag{2.38}$$

$$p_3 = (E_\nu - T, \vec{p}_3) \tag{2.39}$$

$$p_4 = (T + M_A, \vec{p}_4) \tag{2.40}$$

$$q = p_1 - p_3 = p_2 - p_4 = (T, \vec{q}) \tag{2.41}$$

Four vector products:

$$p_3 \cdot p_4 = \frac{1}{2}[(p_3 + p_4)^2 - p_3^2 - p_4^2] = \frac{1}{2}[(p_1 + p_2)^2 - M_A^2] = E_\nu M_A \tag{2.42}$$

$$p_1 \cdot p_2 = E_\nu M_A \tag{2.43}$$

$$p_2 \cdot p_3 = M_A(E_\nu - T) \tag{2.44}$$

$$p_2 \cdot p_4 = M_A(T + M_A) \tag{2.45}$$

$$p_1 \cdot p_3 = (p_3 + p_4 - p_2) \cdot p_3 = M_A T \tag{2.46}$$

$$p_1 \cdot p_4 = p_1 \cdot (p_1 + p_2 - p_3) = M_A(E_\nu - T) \tag{2.47}$$

$$q^2 = (p_1 - p_3)^2 = -2M_A T \tag{2.48}$$

$|\mathscr{M}|^2$ becomes :

$$\mathscr{M}\mathscr{M}^{\dagger} = 32G_F^2 M_A^2 E_\nu^2 Q_W^2 (g_L^\nu)^2 \left(1 - \frac{T}{E_\nu} - \frac{M_A T}{2E_\nu^2}\right) F^2 \tag{2.49}$$

Here T is smaller then E_ν so $\frac{T}{E_\nu}$ term can be neglected

$$|\mathscr{M}|^2 = 32G_F^2 E_\nu^2 M_A^2 Q_W^2 (g_L^\nu)^2 \left(1 - \frac{M_A T}{2E_\nu^2}\right) F(q^2)^2 \tag{2.50}$$

2.3 Differential and Total Cross-Section

2.3.1 $\frac{d\sigma}{dq^2}$ in Lab Frame

Applying Fermi's Golden Rule differential cross-section in lab frame in terms of momentum transfer is take the form:

$$\frac{d\sigma}{dq^2} = -\frac{|\mathscr{M}|^2}{64\pi E_\nu^2 M_A^2} \tag{2.51}$$

The differential cross-section of coherent neutrino-nucleus scattering in Standard Model is given by (Papoulias & Kosmas, 2017)

$$\frac{d\sigma}{dq^2} = \frac{1}{2}\frac{G_F^2}{4\pi}\left[1 - \frac{q^2}{4E_\nu^2}\right]\left[\varepsilon Z F_Z(q^2) - N F_N(q^2)\right]^2 \tag{2.52}$$

where $\varepsilon = 1 - 4sin^2\theta_W$.

2.3.2 $\frac{d\sigma}{dT}$ In Lab Frame

Differential cross-section in terms of T:

The three-momentum transfer is given by $q^2 = 2M_A T + T^2 \simeq 2M_A T$

$$\frac{dq^2}{dT} = 2M_A \tag{2.53}$$

By chain rule

$$\frac{d\sigma}{dT} = 2M_A \left[\frac{d\sigma}{dq^2}\right] \tag{2.54}$$

$$\frac{d\sigma}{dT} = \frac{G_F^2 M_A}{4\pi}\left[1 - \frac{2M_A T}{4E_\nu^2}\right][\varepsilon Z F_Z(2M_A T) - N F_N(2M_A T)]^2 \tag{2.55}$$

2.3.3 Total Cross-Section

The total cross section for coherent neutrino nucleus scattering in terms of T:

$$\sigma_{\nu A} = \int_{T^{min}}^{T^{max}} \left[\frac{d\sigma_{\nu A}}{dT}(T)\right] dT \tag{2.56}$$

Where $T^{min} = 2MT_{min}$ and $T^{max} = 4E_\nu^2[M_A/(M_A + 2E_\nu)] \simeq 4E_\nu^2$. The integration limits are determined by detection of threshold and kinematics, respectively.

CHAPTER THREE
ANALYSIS OF COHERENCY

3.1 Form Factors

The form factor is function which describes the spatial distribution of nucleons inside the nucleus. Weak charge distribution is associated with nucleons. At low energies the wavelength of the Z boson is larger than nucleus dimension. At that limit nucleus can be treated as a point like particle. When three momentum transfer q approaches $1/R$, inner structure of nucleus become important.

The weak form factor can be defined as the Fourier transform of the weak charge distribution of the nucleus $\rho_W(\mathbf{r})$:

$$F(q) \equiv \frac{1}{Q_W} \int \rho_W(\mathbf{r}) e^{i\mathbf{q}\cdot\mathbf{r}} d^3\mathbf{r} \tag{3.1}$$

where q = (T, **q**) is the 4-momentum transfer.

$$Q_W \equiv \int \rho_W(\mathbf{r}) \mathbf{d^3 r} \tag{3.2}$$

An effective method of Ref.(Engel, 1991) can be adopted which assumes neutrons and protons form factors in the same form: $F_N(q^2)$=$F_Z(q^2)$≡$F(q^2)$∈[0,1]. Using $J_1(x)$ as a first order spherical Bessel function and nucleus dependence R_0^2=R^2-5s^2, s=0.5 fm and R=$1.2A^{\frac{1}{3}}$ fm.

$$F(q^2) = [\frac{3}{qR_0}]\, J_1(qR_0)\, \exp[-\frac{1}{2}q^2 s^2] \quad , \tag{3.3}$$

Where $J_1(x)$ is

$$J_1(x) = \frac{sin(x)}{x^2} - \frac{cos(x)}{x} \tag{3.4}$$

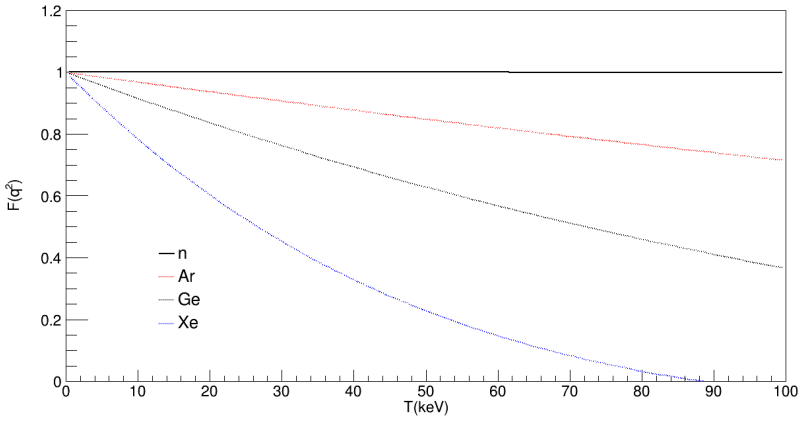

Figure 3.1 The nuclear form factors

3.2 Differential Cross Section

When $T \to 0$ eqn.(2.55) becomes:

$$\frac{d\sigma}{dT}(T \to 0) \simeq [\frac{G_F^2 M_A}{4\pi}][\varepsilon Z - N]^2 \tag{3.5}$$

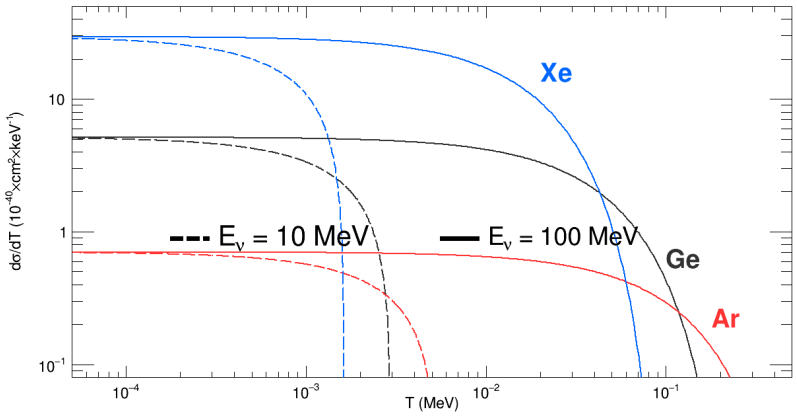

Figure 3.2 Differential cross sections

From Figure (3.2) it is seen that differential cross section and nuclear recoil energy proportional to atomic number of nucleus (A) and incoming neutrino energy (E_ν) . For larger cross section and bigger recoil energies using heavy nuclei is better choice.

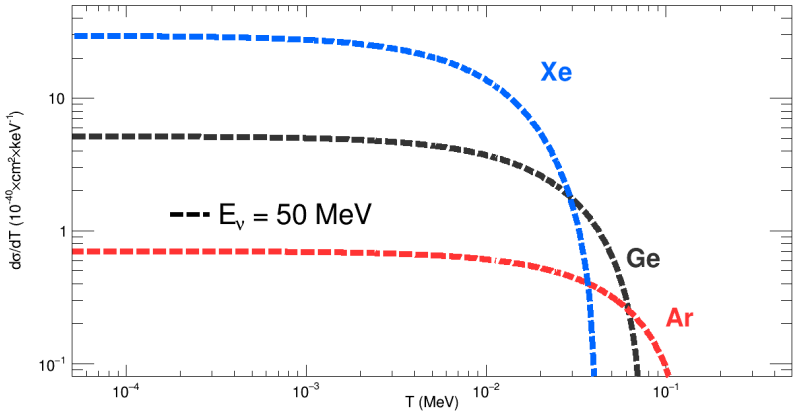

Figure 3.3 Differential cross sections at 50 MeV

3.3 Total Cross Section

When $T \to 0$ eqn.(2.56) becomes:

$$\sigma(T_{min} = 0) = \frac{G_F^2 E_\nu^2}{4\pi} [\varepsilon Z - N]^2 \tag{3.6}$$

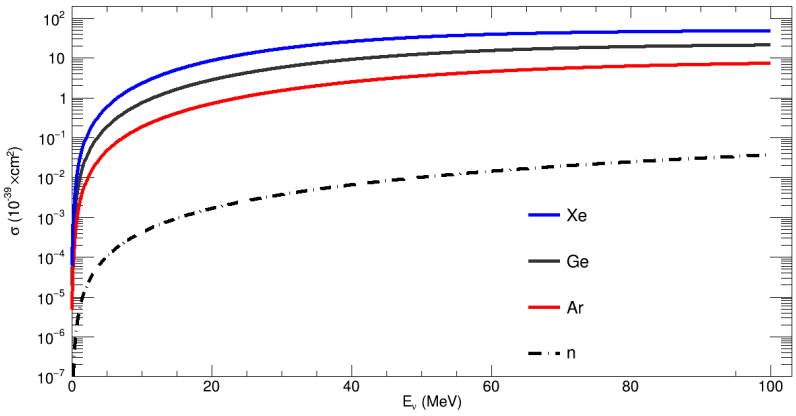

Figure 3.4 Total cross sections

The total cross section enhances with neutron number as seen in equation (3.6).

Neutron rich nuclei are become dominant in the coherent neutrino nucleus scattering. As differential cross section, total cross section is proportional to atomic number and incoming neutrino energy. Figure (3.4) shows that Xe has larger total cross section an Ar has smallest. Neutrons total cross section is illustrated here for later discussion of coherency.

3.4 Coherency

Quantum mechanical coherency can be achieved by adding up nucleons amplitude vectors. Total amplitude $\mathscr{A}$ can be written as (Kerman et al., 2016) :

$$\mathscr{A} = \sum_{j=1}^{Z} e^{i\theta_j} \mathscr{X}_j + \sum_{k=1}^{N} e^{i\theta_k} \mathscr{Y}_k \tag{3.7}$$

where $\mathscr{X}_j(\mathscr{Y}_k)$ stands for the coupling strength and $e^{i\theta_j}$ is the phase factor. $\sigma_{\nu A}$ $(\mathscr{X}_j, \mathscr{Y}_k) = (-\varepsilon, 1)$ for electoweak process. The cross section involves $(Z+N)^2$ terms:

$$\begin{aligned}
\sigma_{\nu A} &\propto \mathscr{A}\,\mathscr{A}^{\dagger} \\
&= \sum_{j=1}^{Z} \mathscr{X}_j^2 + \sum_{k=1}^{N} \mathscr{Y}_k^2 \\
&\quad + \sum_{j=l+1}^{Z} \sum_{l=1}^{Z-1} \left[e^{i(\theta_j-\theta_l)} + e^{-i(\theta_j-\theta_l)} \right] \mathscr{X}_j \mathscr{X}_l \\
&\quad + \sum_{k=m+1}^{N} \sum_{m=1}^{N-1} \left[e^{i(\theta_k-\theta_m)} + e^{-i(\theta_k-\theta_m)} \right] \mathscr{Y}_k \mathscr{Y}_m \\
&\quad + \sum_{j=1}^{Z} \sum_{k=1}^{N} \left[e^{i(\theta_j-\theta_k)} + e^{-i(\theta_j-\theta_k)} \right] \mathscr{X}_j \mathscr{Y}_k \, .
\end{aligned} \tag{3.8}$$

An angle $\langle\Phi\rangle \in [0, \pi/2]$ can be described between any nucleon pairs for decoherence effects.

$$\left[e^{i(\theta_j-\theta_k)}+e^{-i(\theta_j-\theta_k)}\right]=2\cos(\theta_j-\theta_k)=2\cos\langle\Phi\rangle \tag{3.9}$$

To define degree of coherency a parameter α_{coh}, can be defined as : $\alpha_{coh}\equiv\cos\langle\Phi\rangle\in[0,1]$.

The ratio between $\sigma_{\nu A}(Z,N)$ and n(0,1) with assignment of $(\mathscr{X}_j,\mathscr{Y}_k)$ can be written as:

$$\begin{aligned}&\frac{\sigma_{\nu A}(Z,N)}{\sigma_{\nu A}(0,1)} \\ =\ &\{\,\varepsilon^2Z+N+\frac{1}{2}\left[\varepsilon^2Z(Z-1)2\alpha_{coh}\right]+\frac{1}{2}\left[N(N-1)2\alpha_{coh}\right]-\varepsilon ZN2\alpha_{coh}\} \\ =\ &\left\{\alpha_{coh}\left[\varepsilon^2Z(Z-1)+N(N-1)-2\varepsilon ZN\right]+\varepsilon^2+N\right\}\end{aligned} \tag{3.10}$$

When $\alpha_{coh}=1$ full coherency occurs, and while $\alpha_{coh}\to 0$ the coherency vanishes.

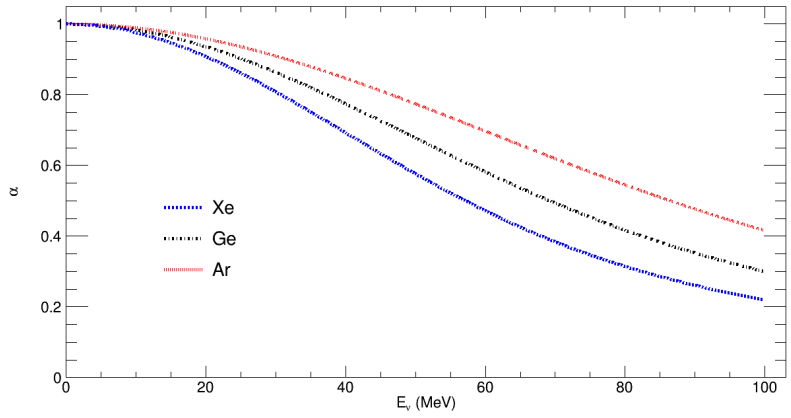

Figure 3.5 Coherency

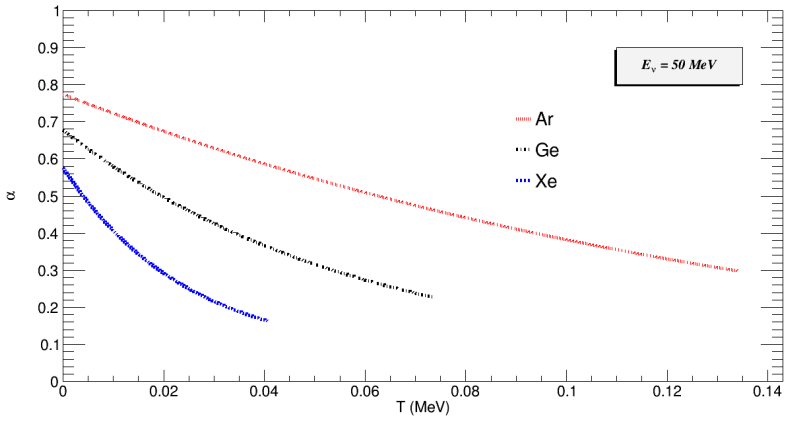

Figure 3.6 Coherency at 50 MeV

In Figure (3.6) the changing of coherency versus nuclear recoil energy is shown. End points correspond to maximum recoils of nucleus. It is seen that lightest nucleus Argon (Ar) has biggest recoil and heaviest nucleus Xenon (Xe) has smallest recoil. From early discussion of total cross it is seen that heavier nuclei has larger cross section. So Germanium (Ge) nucleus between Xenon and Argon seems to be better choice to use as a detector.

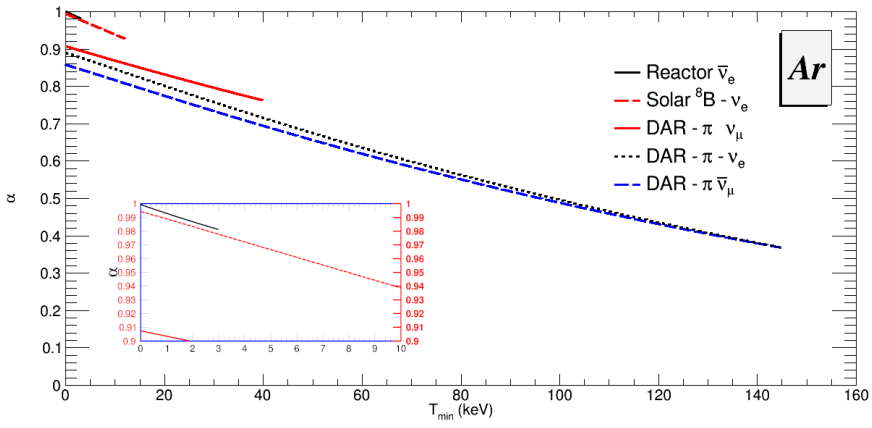

Figure 3.7 Variations of α_{coh} with fluxes for Ar

In Figures (3.7), (3.8), (3.9) known neutrino spectra used for the analysis. The reactor and solar neutrinos give full coherent result. SNS $DAR - \pi$ fluxes give coherency less then 0.9.

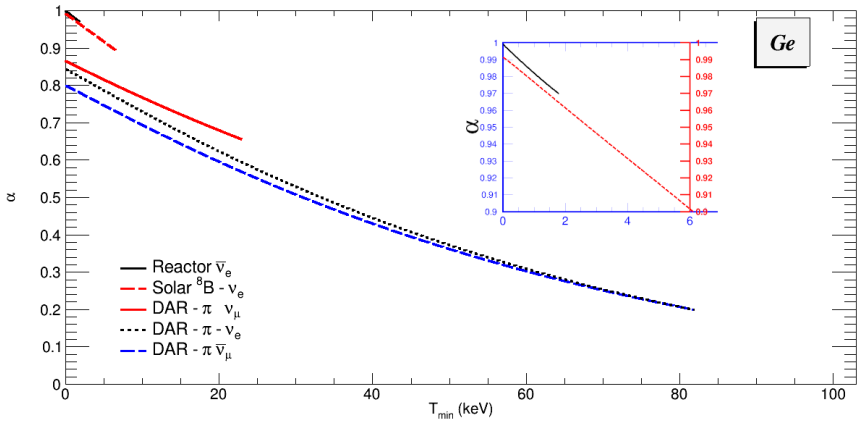

Figure 3.8 Variations of α_{coh} with fluxes for Ge

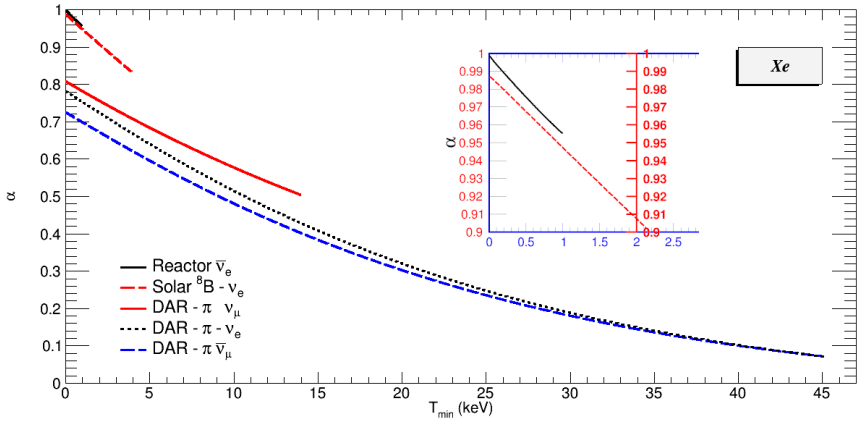

Figure 3.9 Variations of α_{coh} with fluxes for Xe

CHAPTER FOUR
CONCLUSION

With realistic neutrino sources experiments for coherency can be done. Mainly ongoing experiments are using reactor $\bar{\nu_e}$ (Soma et al., 2016) , $DAR_\pi(\nu_\mu, \nu_e, \bar{\nu_\mu})$ (AvignoneIII & Efremenko, 2003) , the solar $\nu_e(^8B)$, and dark matter experiments (Olive et al., 2014).

From our analysis especially the reactor and solar neutrinos achieve the full coherency ($\alpha_{coh} = 1$) at low energy regions (see tables 4.2, 4.3, and 4.4). Mid-range energy DAR-π neutrinos achieve coherency less then $0.9\alpha_{coh}$. The cross section is getting larger with increasing neutrino energy (E_ν) and atomic number (A), but coherency decrease with same conditions (see Table 4.1). Also the contribution of nuclear form factors become less at high energies (See Figure 3.1). From our samples (Ar, Ge, Ze) Ge is the optimum nucleus to work with as a detector in term of high coherency and cross section.

Table 4.1 Degree of coherency with increasing energy

	Ar (α_{coh})	**Ge** (α_{coh})	**Xe** (α_{coh})
$E_\nu = 0 \quad MeV$	1	1	0.999
$E_\nu = 10 \quad MeV$	0.989	0.983	0.975
$E_\nu = 30 \quad MeV$	0.910	0.863	0.807
$E_\nu = 50 \quad MeV$	0.774	0.677	0.576

For future investigations, studies on detecting the process at low energies (up to 15 MeV) can be performed with reactor and solar neutrinos. Also focusing on small detector thresholds is necessary to achieve the goal (sub keV region). New experimental methods need to be improved to study at low energy regions. Achieving detecting the process at low energies will lead to practical usage of detectors as mobile nuclear reactor monitoring.

Table 4.2 Flux contributions to Argon α_{coh}

T_{min} **Ar**	α_{coh} Reactor $\bar{\nu}_e$	α_{coh} Solar ν_e	α_{coh} SNS ν_μ	α_{coh} SNS ν_e	α_{coh} SNS $\bar{\nu}_\mu$
$T_{min} = 0.01 \quad keV$	0.999	0.994	0.907	0.889	0.857
$T_{min} = 3 \quad keV$	0.981	0.977	0.895	0.877	0.845
$T_{min} = 12 \quad keV$	-	0.907	0.861	0.837	0.808
$T_{min} = 40 \quad keV$	-	-	0.762	0.715	0.694
$T_{min} = 145 \quad keV$	-	-	-	0.368	0.367

Table 4.3 Flux contributions to Germanium α_{coh}

T_{min} **Ge**	α_{coh} Reactor $\bar{\nu}_e$	α_{coh} Solar ν_e	α_{coh} SNS ν_μ	α_{coh} SNS ν_e	α_{coh} SNS $\bar{\nu}_\mu$
$T_{min} = 0.01 \quad keV$	0.999	0.991	0.865	0.842	0.799
$T_{min} = 1.8 \quad keV$	0.969	0.964	0.846	0.822	0.780
$T_{min} = 6.7 \quad keV$	-	0.891	0.798	0.766	0.728
$T_{min} = 23 \quad keV$	-	-	0.654	0.593	0.568
$T_{min} = 82 \quad keV$	-	-	-	0.198	0.198

Table 4.4 Flux contributions to Xenon α_{coh}

T_{min} **Xe**	α_{coh} Reactor $\bar{\nu}_e$	α_{coh} Solar ν_e	α_{coh} SNS ν_μ	α_{coh} SNS ν_e	α_{coh} SNS $\bar{\nu}_\mu$
$T_{min} = 0.01 \quad keV$	0.998	0.986	0.807	0.780	0.724
$T_{min} = 1 \quad keV$	0.954	0.947	0.781	0.752	0.698
$T_{min} = 4 \quad keV$	-	0.831	0.707	0.667	0.620
$T_{min} = 14 \quad keV$	-	-	0.503	0.428	0.401
$T_{min} = 45 \quad keV$	-	-	-	0.072	0.072

REFERENCES

Akimov, D., Albert, J., An, P., Awe, C., Barbeau, P., Becker, B. et al. (2017). Observation of coherent elastic neutrino-nucleus scattering. *Science*, *357*(6356), 1123–1126.

AvignoneIII, F. T., & Efremenko, Y. V. (2003, oct). Neutrino–nucleus cross-section measurements at intense, pulsed spallation sources. *Journal of physics g: Nuclear and particle physics*, *29*(11), 2615–2628.

Beringer, J., Arguin, J. F., Barnett, R. M., Copic, K., Dahl, O., Groom, D. E. et al. (2012, Jul). Review of particle physics. *Physical Review D*, *86*, 010001.

Eidelman, S., Hayes, K., Olive, K., Aguilar-Benitez, M., Amsler, C., Asner, D. et al. (2004). Review of particle physics. *Physics Letters B*, *592*(1), 1 - 5. (Review of Particle Physics)

Engel, J. (1991, July). Nuclear form factors for the scattering of weakly interacting massive particles. *Physics Letters B*, *264*, 114-119.

Glashow, S. L. (1961). Partial-symmetries of weak interactions. *Nuclear Physics*, *22*(4), 579–588.

Kerman, S., Sharma, V., Deniz, M., Wong, H., Chen, J.-W., Li, H. et al. (2016). Coherency in neutrino-nucleus elastic scattering. *Physical Review D*, *93*(11), 113006.

Landau, L. (1957). On the conservation laws for weak interactions. *Nuclear Physics*, *3*(1), 127 - 131.

Leader, E., & Predazzi, E. (n.d.). *An Introduction to gauge theories and modern particle physics. Vol. 1: Electroweak interactions, the new particles and the parton model* (Vol. 3). Cambridge: Cambridge University Press.

Lee, T. D., & Yang, C. N. (1957). Parity nonconservation and a two-component theory

of the neutrino. *Physical Review*, *105*, 1671–1675.

Lindner, M., Rodejohann, W., & Xu, X.-J. (2017). Coherent neutrino-nucleus scattering and new neutrino interactions. *Journal of High Energy Physics*, *2017*(3), 97.

Olive, K. A., et al. (2014). Review of particle physics. *Chinese Physics*, *C38*, 090001.

Papoulias, D., & Kosmas, T. (2017). Coherent constraints to conventional and exotic neutrino physics. *Physical Review D*, *97*(arXiv: 1711.09773), 033003.

Peskin, M., & Schroeder, D. (1995). *An introduction to quantum field theory*. New York: Addison-Wesley.

Ramond, P. (2019). Neutrinos and particle physics models. *arXiv preprint arXiv:1902.01741*.

Salam, A. (1957). On parity conservation and neutrino mass. *Il Nuovo Cimento (1955-1965)*, *5*(1), 299–301.

Scholberg, K. (2006). Prospects for measuring coherent neutrino-nucleus elastic scattering at a stopped-pion neutrino source. *physical Review D*, *73*, 033005.

Soma, A., Singh, M., Singh, L., Kumar, G. K., Lin, F., Du, Q. et al. (2016). Characterization and performance of germanium detectors with sub-kev sensitivities for neutrino and dark matter experiments. *Nuclear Instruments and Methods in Physics Research Section A: Accelerators, Spectrometers, Detectors and Associated Equipment*, *836*, 67 - 82.

Thomson, M. (2013). *Modern particle physics*. Cambridge: Cambridge University Press.

Weinberg, S. (1967). A model of leptons. *Physical Review Letters*, *19*, 1264–1266.

APPENDICES

Appendix A: The Standard Model-Electroweak Part

The Standard Model (SM) (Weinberg, 1967) describes the fundamental interactions of elementary particles. It is a gauge theory. Standard Model is builds on $SU(3)_C \times SU(2)_L \times U(1)_Y$ symmetry group. Here C, L, and Y stands for color, left-handed chirality, and weak-hypercharge respectively. This group determines the gauge boson number and interaction type. $SU(3)_C$ generates eight gluons with no mass. $SU(2)_L$ generates the weak charge with massive vector bosons. (W^+ and W^- are charged vector bosons and Z for neutral vector boson). $U(1)_Y$ is photon field generator (γ). In this chapter a short review of the electro-weak part of Standard Model will be given, which is consists of $SU(2)_L$ and $U(1)_Y$ groups, to determine the interactions of neutrinos.

Elementary fermions can be separated in two categories, leptons and quarks, which are shown in Table A.1.

Table A.1 Three fermion generations

	First generation	**Second generation**	**Third generation**
quarks :	up (u)	charm (c)	top (t)
	down (d)	strange (s)	bottom (b)
leptons :	electron neutrino (ν_e)	muon neutrino (ν_μ)	tau neutrino (ν_τ)
	electron (e)	muon (μ)	tau (τ)

Quarks involve all three interactions, strong, weak and electro-magnetic interactions. Leptons involve two interactions and do not involve strong interactions. Quarks are elementary components of hadrons but do not exist as free particles. This means that their masses do not have the usual classical meaning and their values depend on how the masses are defined. The quark masses given in Table A.2 are so-called current

masses, which are the parameters in the QCD Lagrangian. The top quark was discovered in 1994 by the CDF and D0 experiments in Fermilab.

Table A.2 Mass and charge of quarks

Flavor	Mass	Charge (in units of e)
u	1.5-4 MeV	2/3
d	4-8 MeV	-1/3
s	80-130 MeV	-1/3
c	1.15-1.35 GeV	2/3
b	4.1-4.4 GeV	-1/3
t	174.3±5.1 GeV	2/3

Table A.3 Mass and charge of leptons

Flavor	Mass	Charge (e)
e	0.510 MeV	-1
ν_e	<15 eV	0
μ	105.65 MeV	-1
ν_μ	< 190 keV	0
τ	1.777 GeV	-1
ν_τ	< 18.2 MeV	0

A.1 Electroweak Lagrangian

In this section the electroweak part of the SM Lagrangian, which determines neutrino interactions in the SM is presented. Thus, it is adequate to study only the $SU(2)_L \times U(1)_Y$ part of the SM symmetry group. This group has three generators.

$$I_n \tag{A.1}$$
$$(n = 1,2,3).$$

These generators satisfy the angular momentum commutation relations

$$[I_a, I_b] = i\varepsilon_{abc} I_c \tag{A.2}$$

In eqn (A.2) ε_{abc} is the totally anti-symmetric tensor with three indices having $\varepsilon_{123} = \varepsilon_{231} = \varepsilon_{312} = 1$. It is important to note that the nonabelian character of the weak isospin group embodied by th2e commutation relations in eqn (A.2) implies that for each representation of the group the scale of the generators is fixed. For example, in the two-dimensional representation the generators are $I_a = \tau_a/2$, where τ_1, τ_2, τ_3 are the three Pauli matrices. A re-scaling of the generators of the type $I_a \to c_a I_a$ with arbitrary constants c_a would spoil the commutation relations in eqn (A.2). This means that the action of the generators on each representation is unique.

Y is a hyper-charge operator, which generates $U(1)_Y$ group. With the Gell-Mann–Nishijima relation I_3 and the charge operator Q can be combine as:

$$Q = I_3 + \frac{Y}{2} \tag{A.3}$$

This relation is necessary in order to fix the action of the hypercharge operator Y on the fermion fields, which is not constrained by the theory, because the $U(1)_Y$ is abelian. Moreover, the Gell-Mann–Nishijima relation implies the unification of weak and electromagnetic interactions. In order to have local gauge in-variance, one must introduce three vector gauge boson fields A_a^μ (a = 1,2,3) associated with the three generators I_a (a = 1, 2, 3) of the group $SU(2)_L$, and a vector gauge boson B^μ related with the generator Y of the group $U(1)_Y$. The co-variant derivative D_μ, which in gauge theories replaces the normal derivative ∂_μ in the Lagrangian, is defined as :

$$D_\mu = \partial_\mu + ig\mathbf{A}_\mu \cdot \mathbf{I} + ig' B_\mu \frac{Y}{2} \tag{A.4}$$

where the vector notation introduced as:

$$\mathbf{A}_\mu \equiv (A_1^\mu, A_2^\mu, A_3^\mu), \qquad \mathbf{I} \equiv (I_1, I_2, I_3) \tag{A.5}$$

with the scalar product

$$\mathbf{A}_\mu \cdot \mathbf{I} \equiv \sum_{a=1}^{3} A_a^\mu I_a \tag{A.6}$$

The co-variant derivative in eqn (A.4) contains two independent coupling constants: g associated with the group $SU(2)_L$ and g' associated with the group $U(1)_Y$.

The next step in the construction of the electroweak $SU(2)_L \times U(1)_Y$ theory is to choose the representations for the fermion fields. Historically, this choice has been guided by the wisdom of previous experience, in particular the V-A theory of weak interactions and the two-component theory of the neutrino. The left-handed chiral components of the fermion fields are grouped into *weak isospin doublets* .

$$L_L = \begin{pmatrix} \nu_{e_L} \\ e_L \end{pmatrix}, \tag{A.7}$$

$$Q_L = \begin{pmatrix} u_L \\ d_L \end{pmatrix} \tag{A.8}$$

From the choice in eqn (A.7) of the weak isospin representation of the fermion fields, the generators of the $SU(2)_L$ group are fixed to be $I_a = \tau/2$:

$$\mathbf{I}L_L = \frac{\tau}{2} L_L, \tag{A.9}$$

$$\mathbf{I}Q_L = \frac{\tau}{2} Q_L \tag{A.10}$$

where $\tau = (\tau_1, \tau_2, \tau_3)$. On the other hand, the action of the hypercharge operator Y is

fixed by the Gell-Mann–Nishijima relation in eqn (A.3) :

$$YL_L = -L_L, \tag{A.11}$$

$$YQ_L = \frac{1}{3}Q_L \tag{A.12}$$

Hence, the left-handed lepton and quark doublets have, respectively, hypercharge Y = -1 and Y = 1/3.

The elements g of the group of local $SU(2)_L \times U(1)_Y$ transformations with a set of 3+1 parameters $(\theta(x), \eta(x))$, where $\theta(x) = \theta_1(x), \theta_2(x), \theta_3(x)$ are parameterized, which depend on space-time x:

$$g(\theta(x), \eta(x)) \in SU(2)_L \times U(1)_Y \tag{A.13}$$

with unitary representation of $g(\theta(x), \eta(x))$ on the vector space of the fields

$$U(\theta(x), \eta(x)) = e^{i\theta(x)\cdot\mathbf{I} + i\eta(x)\frac{Y}{2}} = U(\theta(x))U(\eta(x)) \tag{A.14}$$

with

$$U(\theta(x)) = e^{i\theta(x)\cdot\mathbf{I}} \tag{A.15}$$

$$U(\eta(x)) = e^{i\eta(x)\frac{Y}{2}} \tag{A.16}$$

The transformation of the left-handed fermion doublets under $g(\theta(x), \eta(x))$ is given by

$$L_L \xrightarrow{g(\theta(x),\eta(x))} L'_L = U(\theta(x), \eta(x))L_L = U^l_L(\theta(x), \eta(x))L_L \tag{A.17}$$

$$Q_L \xrightarrow{g(\theta(x),\eta(x))} Q'_L = U(\theta(x), \eta(x))Q_L = U^q_L(\theta(x), \eta(x))Q_L \tag{A.18}$$

where

$$U_L^l(\theta(x),\eta(x)) = e^{\frac{i}{2}\theta\cdot\tau-\frac{i}{2}\eta(x)}, \tag{A.19}$$

$$Q_L^q(\theta(x),\eta(x)) = e^{\frac{i}{2}\theta\cdot\tau+\frac{i}{6}\eta(x)} \tag{A.20}$$

In the Standard Model, the neutrino fields have only left-handed components. This assumption follows from the two-component theory of Landau (Landau, 1957), Lee and Yang (Lee & Yang, 1957), and Salam (Salam, 1957), implying that neutrinos are massless. The right-handed components of the other fermions,

$$e_R, \tag{A.21}$$

$$u_R, \tag{A.22}$$

$$d_R \tag{A.23}$$

are assumed to be singlets under the weak isospin group of transformations:

$$f_R = 0 \tag{A.24}$$

$$(f = e,u,d) \tag{A.25}$$

From the Gell-Mann–Nishijima relation in eqn(A.3) e_R, u_R, and d_R have, respectively, hypercharge Y = -2, 4/3, -2/3:

$$Ye_R = -2e_R, \tag{A.26}$$

$$Yu_R = \frac{4}{3}u_R, \tag{A.27}$$

$$Yd_R = -\frac{2}{3}d_R, \tag{A.28}$$

Then, the transformation of the right-handed components of the fermion fields under the transformation in eqn (A.13) is given by

$$f_R \xrightarrow{g(\theta(x),\eta(x))} f_R' = U(\theta(x),\eta(x))f_R = u_R^f(\eta(x))f_R \tag{A.29}$$

$$(f = e,u,d) \tag{A.30}$$

where

$$U_R^e(\eta(x)) = e^{-i\eta(x)}, \tag{A.31}$$

$$U_R^d(\eta(x)) = e^{-\frac{1}{3}i\eta(x)}, \tag{A.32}$$

$$U_R^u(\eta(x)) = e^{\frac{2}{3}i\eta(x)} \tag{A.33}$$

Table A.4 Hypercharge and weak iso-spin values

		I	I_3	**Y**	**Q**
Lepton Doublet	$L_L = \begin{pmatrix} \nu_{e_L} \\ e_L \end{pmatrix}$	1/2	1/2 , -1/2	-1	0, -1
Lepton Singlet	e_R	0	0	-2	-1
Quark Doublet	$Q_L = \begin{pmatrix} u_L \\ d_L \end{pmatrix}$	1/2	1/2 , -1/2	1/3	2/3, -1/3
Quark Singlets	u_R, d_R	0	0	4/3, -2/3	2/3, -1/3

The values of the hypercharge, weak isospin, and electric charge of the fermion singlets and doublets are listed in Table A.4.

The electroweak SM Lagrangian is the most general renormalizable Lagrangian invariant under the local symmetry group $U(2)_L \times U(1)_Y$ written in terms of the fermion fields, for the first generation of leptons and quarks :

$$\begin{aligned}
\mathscr{L} &= i\overline{L_L}\not{D}L_L + i\overline{Q_L}\not{D}Q_L + \sum_{f=e,u,d} i\overline{f_R}\not{D}f_R \\
&- \frac{1}{4}A_{\mu\nu}A^{\mu\nu} - \frac{1}{4}B_{\mu\nu}B^{\mu\nu} \\
&+ (D_\mu\Phi)^\dagger(D_\mu\Phi) - \mu^2\Phi^\dagger\Phi - \lambda(\Phi^\dagger\Phi)^2 \\
&- y^e(\overline{L_L}\Phi_{e_R} + \overline{e_R}\Phi^\dagger L_L) \\
&- y^d(\overline{Q_L}\Phi_{d_R} + \overline{d_R}\Phi^\dagger Q_L) - y^u(\overline{Q_L}\tilde{\Phi}_{u_R} + \overline{u_R}\tilde{\Phi}^\dagger Q_L)
\end{aligned} \tag{A.34}$$

The second line contains the kinetic terms and self-couplings of the gauge bosons. The

third line is the Lagrangian of the Higgs field which generates the spontaneous symmetry breaking. The fourth and fifth lines describe the Higgs–fermion Yukawa couplings which generate lepton masses.

Let us consider only the first line in eqn (A.34). Since under the transformation in eqn (A.13) the lepton and quark fields transform according to eqns (A.17), (A.18), and (A.29), in order to satisfy gauge invariance, the covariant derivative must transform as

$$D_\mu \xrightarrow{g(\theta(x),\eta(x))} D'_\mu = U(\theta(x),\eta(x)) D_\mu U^{-1}(\theta(x),\eta(x)) \tag{A.35}$$

This means that the gauge boson fields transform as

$$\mathbf{A}_\mu \cdot \mathbf{I} \xrightarrow{g(\theta(x),\eta(x))} \mathbf{A}'_\mu \cdot \mathbf{I} = U(\theta(x)) \left[\mathbf{A}_\mu \cdot \mathbf{I} - \frac{i}{g} \partial_\mu \right] U^{-1}(\theta(x)) \tag{A.36}$$

$$B_\mu \frac{Y}{2} \xrightarrow{g(\theta(x),\eta(x))} B'_\mu \frac{Y}{2} = U(\eta(x)) \left[B_\mu \frac{Y}{2} - \frac{i}{g'} \partial_\mu \right] U^{-1}(\eta(x)) \tag{A.37}$$

The transformation of the B_μ field can be simplified to

$$B_\mu \xrightarrow{g(\theta(x),\eta(x))} B'_\mu = B_\mu - \frac{i}{g'} \partial_\mu \tag{A.38}$$

which is similar to the transformation under local $U(1)_Q$ transformations of the electromagnetic field in QED [see, for example, (Leader & Predazzi, 2011)].

A.2 Electroweak Interactions

Expanding the covariant derivatives in the first line of eqn (A.34) and omitting the kinetic terms, the interaction Lagrangian that describes the coupling of the fermions

with the gauge bosons is obtained as :

$$\begin{aligned}\mathscr{L}_I &= -\frac{1}{2}\overline{L_L}\left(g\not{\mathbf{A}}\cdot\tau - g'\not{B}\right)L_L - \frac{1}{2}\overline{Q_L}\left(g\not{\mathbf{A}}\cdot\tau + \frac{1}{3}g'\not{B}\right)Q_L \\ &+ g'\overline{e_R}\not{B}e_R - \frac{2}{3}g'\overline{u_R}\not{B}u_R + \frac{1}{3}g'\overline{d_R}\not{B}d_R\end{aligned} \tag{A.39}$$

In order to derive the explicit interaction terms for the fermions, let us first consider the leptons only :

$$\mathscr{L}_{I,L} = \frac{1}{2}(\overline{\nu_{e_L}} \quad \overline{e_L}) \begin{pmatrix} g\not{A}_3 - g'\not{B} & g(\not{A}_1 - i\not{A}_2) \\ g(\not{A}_1 + i\not{A}_2) & -g\not{A}_3 - g'\not{B} \end{pmatrix} \begin{pmatrix} \nu_{e_L} \\ e_L \end{pmatrix} + g'\overline{e_R}\not{B}e_R \tag{A.40}$$

Now separate this interaction Lagrangian into charged-current (CC) Lagrangian

$$\mathscr{L}^{CC}_{I,L} = -\frac{g}{2}\overline{\nu_{e_L}}(\not{A}_1 - i\not{A}_2)e_L + \overline{e_L}(\not{A}_1 + i\not{A}_2)\nu_{eL} \tag{A.41}$$

which is given by the off-diagonal terms in eqn (A.40), and a neutral-current (NC) Lagrangian

$$\mathscr{L}^{NC}_{I,L} = -\frac{1}{2}\overline{\nu_{eL}}(g\not{A}_3 - g'\not{B})e_L - 2g'\overline{e_R}\not{B}e_R \tag{A.42}$$

given by the diagonal terms in eqn (A.40). Now, let us consider first the charged-current Lagrangian in eqn (A.41). Defining a field that annihilates W^+ bosons and creates W^- bosons as W^μ :

$$W^\mu \equiv \frac{A^\mu_1 - iA^\mu_2}{\sqrt{2}} \tag{A.43}$$

then

$$\begin{aligned}\mathscr{L}_{I,L}^{CC} &= -\frac{g}{\sqrt{2}}\overline{\nu_{eL}}\not{W}e_L + \overline{e_L}\not{W}^{\dagger}\nu_{e_L} \\ &= -\frac{g}{2\sqrt{2}}\overline{\nu_e}\gamma^{\mu}(1-\gamma^5)eW_{\mu} + Hc. \\ &= -\frac{g}{2\sqrt{2}}j_{W,L}^{\mu}W_{\mu} + Hc.\end{aligned} \tag{A.44}$$

where $j_{W,L}^{\mu}$ is the leptonic charged current

$$j_{W,L}^{\mu} = \overline{\nu_e}\gamma^{\mu}(1-\gamma^5)e = 2\overline{\nu_{e_L}}\gamma^{\mu}e_L \tag{A.45}$$

The interaction Lagrangian in eqn (3.32) generates the trilinear couplings represented by the diagrams

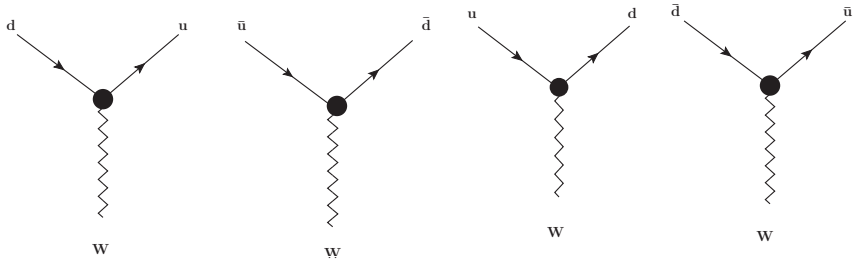

Figure A.1 Trilinear couplings

The first two diagrams are generated by the term $j_{W,L}^{\mu}W_{\mu}$, and and the last two by the Hermitian-conjugated term $j_{W,L}^{\mu\dagger}W_{\mu}^{\dagger} = \overline{e}\gamma^{\mu}(1-\gamma^5)\nu_e W_{\mu}^{\dagger}$.

Next consider the neutral-current Lagrangian in eqn (A.42). The theory must include the electromagnetic interactions described by the quantum electrodynamic (QED) Lagrangian

$$\mathscr{L}_{I,L}^{(\gamma)} = -ej_{\gamma,L}^{\mu}A_{\mu} \tag{A.46}$$

where e is the elementary electric charge, A^{μ} is electromagnetic field, and $j_{\gamma,L}^{\mu}$ is the

leptonic electromagnetic current

$$j^{\mu}_{\gamma,L} = -\bar{e}\gamma^{\mu}e \tag{A.47}$$

The minus sign is due to the negative charge of the electron. The QED Lagrangian can be obtained as part of the neutral-current Lagrangian in eqn (A.42) expressing the electromagnetic field A^{μ} as an appropriate linear combination of A^{μ}_3 and B^{μ}. Let boson field Z^{μ} , performing a rotation in the plane of the A^{μ}_3 , B^{μ} fields through an angle θ_W:

$$A^{\mu} = sin\theta_W A^{\mu}_3 + cos\theta_W B^{\mu} \tag{A.48}$$

$$Z^{\mu} = cos\theta_W A^{\mu}_3 - sin\theta_W B^{\mu} \tag{A.49}$$

The angle θ_W is called the weak mixing angle or Weinberg angle (Weinberg, 1967). The weak mixing angle is chosen in order to obtain the QED Lagrangian for the coupling between the electromagnetic field and the fermion fields. Inserting the expressions in eqns (A.48) and (A.49) in the neutral-current Lagrangian in eqn (A.42), it takes the form :

$$\begin{aligned} \mathscr{L}^{NC}_{I,L} = & - \frac{1}{2}\{\overline{\nu_{eL}}[(gcos\theta_W + g'sin\theta_W)\not{Z} + (gsin\theta_W - g'cos\theta_W)\not{A}]\nu_{e_L} \\ & - \overline{e_L}[(gcos\theta_W - g'sin\theta_W)\not{Z} + (gsin\theta_W + g'cos\theta_W)\not{A}]e_L \\ & - 2g'\overline{e_R}[-sin\theta_W\not{Z} + cos\theta_W\not{A}]e_R\} \end{aligned} \tag{A.50}$$

Since neutrinos are neutral particles, they do not have a coupling to the electro-magnetic field. Setting the coefficient of the corresponding term in eqn (A.50) to zero, it takes the form:

$$gsin\theta_W = g'cos\theta_W \Rightarrow tan\theta_W = \frac{g'}{g} \tag{A.51}$$

This is an important relation, which connects the coupling constants g and g' of the SM with the weak mixing angle θ_W .

Substituting eqn (A.51) into eqn (A.50) :

$$\begin{aligned}\mathscr{L}_{I,L}^{NC} = & - \frac{g}{2cos\theta_W}\{\overline{\nu_{eL}}\not{Z}\nu_{eL} - (1-2sin^2\theta_W)\overline{e_L}\not{Z}e_L + 2sin^2\theta_W\overline{e_R}\not{Z}e_R\} \\ & + gsin\theta_W\bar{e}\not{A}e\end{aligned} \tag{A.52}$$

Since the last term gives the coupling of the electron field with the electromagnetic field, it must coincide with the QED interaction Lagrangian in eqn (A.46) :

$$gsin\theta_W = e \tag{A.53}$$

Using the relation in eqn (A.51) :

$$g'cos\theta_W = e \tag{A.54}$$

These two relations are very important, because they give the relation between the coupling constants g and g' and the elementary electric charge e.

The neutral-current Lagrangian can be written as

$$\mathscr{L}_{I,L}^{(NC)} = \mathscr{L}_{I,L}^{(Z)} + \mathscr{L}_{I,L}^{(\gamma)} \tag{A.55}$$

where $\mathscr{L}_{I,L}^{(\gamma)}$ is the QED Lagrangian in eqn (A.46) and $\mathscr{L}_{I,L}^{(Z)}$ is the weak neutral-current Lagrangian given by

$$\mathscr{L}_{I,L}^{(Z)} = -\frac{g}{2cos\theta_W} j_{Z,L}^{\mu} Z_{\mu} \tag{A.56}$$

with the leptonic weak neutral-current

$$j_{Z,L}^{\mu} = 2g_L^{\nu}\overline{\nu_{eL}}\gamma^{\mu}\nu_{eL} + 2g_L^{l}\overline{e_L}\gamma^{\mu}e_L + 2g_R^{l}\overline{e_R}\gamma^{\mu}e_R \tag{A.57}$$

Here, the coefficients g_L^ν, g_L^l, and g_R^l (the superscript l indicates a charged lepton) whose values, obtained from eqn (A.52), are given in Table 3.6.

In general, the values of the coefficients g_L^f and g_R^f for a fermion field f are given by

$$g_L^f = I_3^f - q_f sin^2\theta_W \tag{A.58}$$

$$g_R^f = -q_f sin^2\theta_W \tag{A.59}$$

where I_3^f is the value of the third component of the weak isospin and q_f is the electric charge of the fermion in units of the elementary electric charge e (see Table 3.5).

Because of the mixing of the gauge fields A_3^μ and B^μ in eqns (A.48) and (A.49), one can see that the weak neutral-current interactions of charged fermion fields involve not only their left-handed component, but also the right-handed one, with a strength proportional to the electric charge and to $sin\theta_W$.

The leptonic weak neutral current in eqn (A.57) can also be written as

$$j_{Z,L}^\mu = \overline{\nu_e}\gamma^\mu \left(g_V^\nu - g_A^\nu \gamma^5\right) \nu_e + \overline{e}\gamma^\mu \left(g_V^l - g_A^l \gamma^5\right) e \tag{A.60}$$

where the widely used vector and axial couplings $g_V^{\nu,l}$ and $g_A^{\nu,l}$ for neutrinos and charged leptons, whose values are given in Table (A.5). In general, the values of g_V^f and g_A^f for a fermion field f are given by

$$g_V^f = g_L^f + g_R^f = I_3^f - 2q_f sin^2\theta_W \tag{A.61}$$

$$g_A^f = g_L^f - g_R^f = I_3^f \tag{A.62}$$

Table A.5 Values of g_L, g_R, g_V, g_A for the fermion fields

Fermions	g_L	g_R	g_v	g_A
ν_e, ν_μ, ν_τ	$g_L^\nu = \frac{1}{2}$	$g_R^\nu = 0$	$g_V^\nu = \frac{1}{2}$	$g_A^\nu = \frac{1}{2}$
e, μ, τ	$g_L^l = -\frac{1}{2} + s_W^2$	$g_R^l = s_W^2$	$g_V^l = -\frac{1}{2} + 2s_W^2$	$g_A^l = -\frac{1}{2}$
u, c, t	$g_L^U = \frac{1}{2} - \frac{2}{3}s_W^2$	$g_R^U = -\frac{2}{3}s_W^2$	$g_V^U = \frac{1}{2} - \frac{4}{3}s_W^2$	$g_A^U = \frac{1}{2}$
d, s, b	$g_L^D = -\frac{1}{2} + \frac{1}{3}s_W^2$	$g_R^D = \frac{1}{3}s_W^2$	$g_V^D = -\frac{1}{2} + \frac{2}{3}s_W^2$	$g_A^D = -\frac{1}{2}$